

Regulated Assembly of the Transenvelope Protein Complex Required for Lipopolysaccharide Export

Elizaveta Freinkman,[†] Suguru Okuda,[‡] Natividad Ruiz,[§] and Daniel Kahne^{*,‡,||}

[†]Chemical Biology Graduate Program and [‡]Department of Chemistry and Chemical Biology, Harvard University, 12 Oxford Street, Cambridge, Massachusetts 02138, United States

[§]Department of Microbiology, The Ohio State University, 484 West 12th Avenue, Columbus, Ohio 43210, United States

^{||}Department of Biological Chemistry and Molecular Pharmacology, Harvard Medical School, 45 Shattuck Street, Boston, Massachusetts 02115, United States

S Supporting Information

ABSTRACT: Gram-negative bacteria are impervious to many drugs and environmental stresses because they possess an outer membrane (OM) containing lipopolysaccharide (LPS). LPS is biosynthesized at the cytoplasmic (inner) membrane and is transported to the OM by an unknown mechanism involving the LPS transport proteins, LptA–G. These proteins have been proposed to form a bridge between the two membranes; however, it is not known how this bridge is assembled to prevent mistargeting of LPS. We use in vivo photo-cross-linking to reveal the specific protein–protein interaction sites that give rise to the Lpt bridge. We also show that the formation of this transenvelope bridge cannot proceed before the correct assembly of the LPS translocon in the OM. This ordered sequence of events may ensure that LPS is never transported to the OM if it cannot be translocated across it to the cell surface.



The cell envelope of Gram-negative bacteria is characterized by the presence of an outer membrane (OM) surrounding the cytoplasmic (inner) membrane (IM) and the peptidoglycan cell wall (Figure 1). The OM is a unique asymmetric

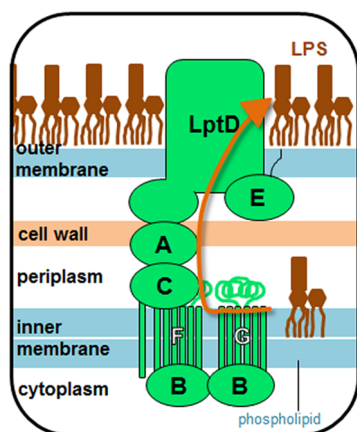


Figure 1. The lipopolysaccharide exporter consists of seven essential proteins, LptA–G, that form a transenvelope complex spanning the inner membrane (IM), periplasm, and outer membrane (OM).

bilayer with an inner leaflet consisting of phospholipid and an outer leaflet consisting of lipopolysaccharide (LPS).^{1–3} Anionic LPS molecules are bridged by divalent cations in vivo to create an impervious layer that blocks the influx of hydrophobic molecules, such as antibiotics, bile salts, and detergents.⁴ LPS is

biosynthesized at the cytoplasmic face of the IM⁵ and then flipped to the periplasmic side by MsbA.⁶ Subsequently, the molecule is transported across the periplasm and the OM and positioned exclusively at the cell surface.

In *Escherichia coli*, this LPS transport process is known to require the seven essential Lpt proteins,⁷ but how these proteins move large, amphipathic LPS molecules across both membranes and the periplasmic space is not understood. The Lpt proteins are localized in three distinct compartments of the cell envelope (Figure 1). In the IM, LptB, -F, and -G comprise an ATP-binding cassette (ABC) transporter that is proposed to facilitate release of LPS from the IM. LptB, -F, and -G associate with LptC, an integral IM protein whose function is not well understood.^{8–11} In the OM, LptD^{12,13} consists of a large N-terminal periplasmic domain of unknown function and a C-terminal transmembrane β -barrel domain that binds lipoprotein LptE.^{14–16} In its functional form, LptD contains two interdomain disulfide bonds whose proper formation requires LptE, but which are not required for the stability of the LptD–LptE complex.^{16–18} The LptD–LptE complex is proposed to serve as the translocon that facilitates the passage of LPS across the OM bilayer.

LPS has been suggested to transit the aqueous periplasmic space via a transenvelope bridge. In support of this hypothesis, LPS transport has been observed in spheroplasts, bacterial cells in which the soluble periplasmic contents have been lost.¹⁹

Received: May 7, 2012

Revised: June 3, 2012

Published: June 5, 2012



Moreover, all seven Lpt proteins cofractionate and copurify, suggesting that they are found in a single complex.²⁰ Depletion of any Lpt protein causes the accumulation of LPS at the periplasmic face of the IM,⁹ consistent with a model in which all seven proteins function in a highly cooperative manner to prevent mistargeting of LPS by defective transport machines. It is not known how the Lpt proteins are assembled into a trans-envelope structure that ensures proper LPS export.

In this work, we establish the architecture of the trans-envelope Lpt bridge in vivo. We define the interaction sites of the periplasmic protein LptA with LptC in the IM and with the N-terminal domain of LptD in the OM. These structurally homologous domains interact in a conserved manner involving the edges of their β -sheets. We also establish how the assembly of this bridge is regulated. We demonstrate that formation of the Lpt bridge requires the presence of correct disulfide bonds in LptD, which itself depends on the proper assembly of the LptD–LptE translocon in the OM. This regulatory mechanism may prevent mistargeting of LPS by Lpt complexes that are not fully functional.

EXPERIMENTAL PROCEDURES

In Vivo Photo-Cross-Linking and Whole-Cell Lysate Analysis. To construct *E. coli* strains for in vivo photo-cross-linking, we replaced specific codons within the *lptA*, *lptC*, and *lptD* sequences with the TAG codon and used amber suppression to incorporate the UV photo-cross-linkable unnatural amino acid *p*-benzoylphenylalanine (*p*BPA) at these positions^{21,22} (see the Supporting Information for details of strain construction). Diploid strains were used for all experiments except where otherwise noted. Overnight cultures grown in LB supplemented with *p*BPA and antibiotics, as appropriate, were diluted 1:100 into 100 mL of the same medium and grown to midlog phase at 37 °C. Each culture was split in half, and each sample was pelleted and either used directly or resuspended in 10 mL of ice-cold TBS [20 mM Tris (pH 8.0) and 150 mM NaCl] and irradiated with UV light at 365 nm for 10 min in an LM-26 benchtop transilluminator (UVP). All cells were resuspended in 2.5 mL of ice-cold TBS-B [20 mM Tris (pH 8.0), 300 mM NaCl, and 20 mM imidazole] containing 1% Anzergent 3-14 (Anatrace), 100 μ g/mL lysozyme, 1 mM phenylmethanesulfonyl fluoride (PMSF), and 50 μ g/mL DNase I, lysed by sonication, and centrifuged at 18500g in a table-top centrifuge for 30 min. Nickel affinity purification was performed as described previously.¹⁵ Eluates were concentrated to a final volume of approximately 40 μ L using 10000 Da cutoff Amicon centrifugal concentrators (Millipore). Sodium dodecyl sulfate–polyacrylamide gel electrophoresis (SDS–PAGE) buffer was added to a final volume of 80 μ L for SDS–PAGE and immunoblotting. Sample loading was normalized by cell density except where stated otherwise.

In Vivo Photo-Cross-Linking and Total Membrane Analysis. Cell cultures (1.5 L) were grown, harvested, and UV-irradiated (or not) as described in the previous section. All samples were resuspended in 10 mL of ice-cold TBS supplemented with 100 μ g/mL lysozyme, 1 mM PMSF, and 50 μ g/mL DNase I. Cells were lysed and membranes collected, extracted, and subjected to TALON affinity chromatography as described previously.²⁰ The final eluates were concentrated to ~150 μ L using a 3000 Da cutoff filter (Millipore), and samples were mixed with an equal volume of SDS–PAGE buffer for SDS–PAGE and immunoblotting.

Additional Methods. Bacterial strains, constructs, antibodies, antibiotics, SDS–PAGE, and other experimental methods are described in the Supporting Information.

RESULTS

The Lpt Bridge Forms a Head-to-Tail Oligomer of Structurally Homologous Domains in Vivo. We have previously suggested that the Lpt proteins form a single complex that spans the IM, periplasm, and OM.²⁰ Here, we have used in vivo photo-cross-linking to define which proteins form this trans-envelope bridge and how they are connected. To do this, we used *E. coli* strains in which proteins substituted with the UV photo-cross-linkable residue *p*BPA^{21,22} were expressed at low levels. Each of these modified proteins could support cell growth in the absence of the relevant wild-type chromosomal allele, establishing that they are functional. By testing a variety of positions within each protein of interest, we could map the sites at which it interacts with other members of the Lpt assembly in vivo.

We initially focused on LptA. This protein has been proposed to physically link the IM and the OM because it is the only periplasmic Lpt component without a membrane tether and because it fractionates with both membranes.²⁰ Also, one intermolecular interaction of LptA has already been established: LptA is copurified with overexpressed LptC,²³ and when purified separately, the two proteins stably associate.²⁴ To determine if our in vivo photo-cross-linking system could identify specific sites of interaction between LptA and LptC, we generated variants of His-tagged LptA (LptA-His) substituted with *p*BPA at 14 sites distributed throughout the three-dimensional structure of LptA.²⁵ Upon coexpression of these variants with FLAG-tagged LptC (FLAG-LptC), we observed robust in vivo photo-cross-linking between FLAG-LptC and LptA-His substituted with *p*BPA at position H37 (Figure 2A and Figure S1 of the Supporting Information). This result shows that the N-terminal end of LptA (Figure 2C) physically interacts with LptC in the Lpt complex in vivo.

Having shown that LptA–LptC interactions can be detected by in vivo photo-cross-linking, we sought to identify the residues of LptC responsible for the interaction with LptA. We tested 23 positions distributed throughout the three-dimensional structure of LptC (Figure S2 of the Supporting Information)²⁶ and found that LptC substituted with *p*BPA at position A172 or Y182 could be cross-linked to LptA in vivo (Figure 2B and Figure S2 of the Supporting Information). These LptA-interacting residues are found at the C-terminal edge of the LptC β -jellyroll (Figure 2C), consistent with the previous observation that mutants in the C-terminus of LptC disrupt the association with LptA.²³ Thus, LptC and LptA interact via their C- and N-terminal edges, respectively (Figure 2C), in a manner similar to the interactions within LptA oligomers in the crystal structure of LptA.²⁵ These observations explain how LptA is anchored at the IM.

Whereas interactions between LptA and LptC at the IM had been observed previously, nothing was known about how LptA is anchored at the OM. During our survey of potential interaction sites throughout LptA, we observed that LptA-His-V163*p*BPA could form a cross-linked product of >100 kDa (Figure S1 of the Supporting Information). This molecular mass is consistent with a covalent adduct of LptA-His (18 kDa) and LptD (87 kDa). Indeed, immunoblotting with α LptD antiserum confirmed strong cross-linking between LptA-His and LptD (Figure 2D). Thus, while the N-terminus of LptA interacts with LptC at the IM, the C-terminus of LptA interacts with LptD at the OM (Figure 2C). However, these results do not clarify

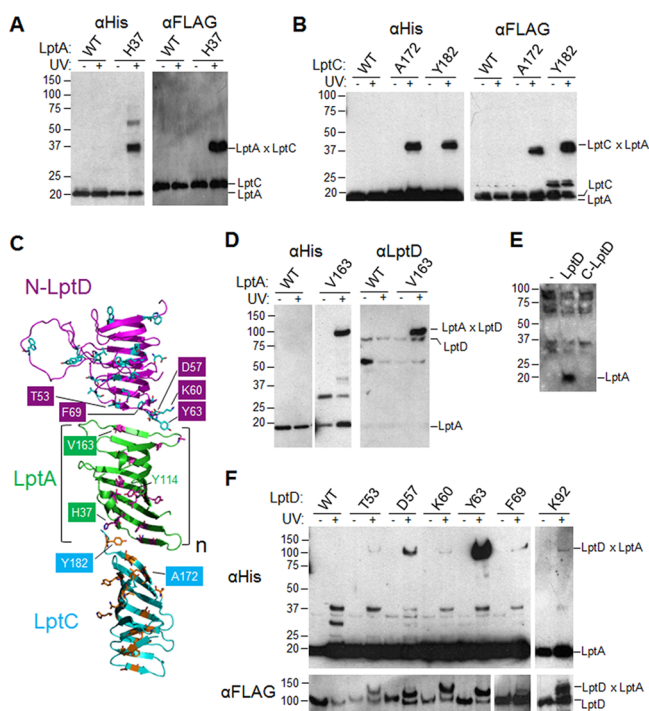


Figure 2. The Lpt bridge is an oligomer of structurally homologous domains: LptC, LptA, and the N-terminal domain of LptD. (A) *E. coli* cells expressing low levels of N-terminally FLAG-tagged LptC (FLAG-LptC) and either wild-type C-terminally His-tagged LptA (LptA-His) or LptA-His containing pBPA at position H37 (numbering includes the LptA signal sequence, amino acids 1–27) were either left untreated or irradiated with UV light. After cell lysis, nickel affinity chromatography, and SDS–PAGE, samples were blotted with either α His (left) or α FLAG (right) antibodies. See Figure S1 of the Supporting Information. (B) Cells expressing LptA-His and the indicated pBPA-substituted variant of FLAG-LptC were treated as described for panel A. See Figure S2 of the Supporting Information. (C) To model the interactions within the Lpt bridge, one monomer in the tetrameric crystal form of LptA²⁵ was manually replaced with the crystal structure of LptC (cyan),²⁶ while another monomer was replaced with a model structure of N-LptD (magenta), generated by HHPred and MODELER⁴¹ on the basis of the LptA structure. The LptC, LptA, and LptD residues analyzed here and in Figures S1–S3 of the Supporting Information are shown in contrasting colors, and residues where cross-linking was observed are labeled. The number (n) of LptA molecules present in the bridge remains unclear (see the text). (D) Cells expressing the indicated pBPA-substituted LptA-His variant were either left untreated or irradiated with UV light. Membrane extracts from each cell sample were subjected to TALON affinity chromatography, followed by immunoblotting with the indicated antibodies. (E) Membrane extracts from cells expressing full-length LptD-His, C-LptD-His (where C-LptD denotes amino acids 203–784, equipped with the native LptD N-terminal signal sequence, amino acids 1–24), or neither (–) were subjected to TALON affinity chromatography, followed by immunoblotting with the α LptA antibody. (F) Cells expressing LptA-His and the indicated pBPA-substituted variants of full-length LptD-3XFLAG (numbering includes the LptD signal sequence, amino acids 1–24) were treated and analyzed as described for panel A. Sample loading for the α FLAG blot was adjusted to compensate for the unequal translation efficiency of various pBPA-containing protein constructs. See Figure S3 of the Supporting Information.

whether a single LptA molecule can engage in both interactions simultaneously (vide infra).

LptD consists of a periplasmic N-terminal domain (N-LptD) and a C-terminal transmembrane β -barrel domain (C-LptD).¹⁵

We asked which of these domains serves as the OM anchor for LptA. We previously showed that isolated C-LptD is folded because it can associate with LptE as efficiently as full-length LptD.¹⁵ By contrast, we found that, unlike full-length LptD, isolated C-LptD did not associate with LptA (Figure 2E). Thus, elements of N-LptD are required for the interaction between LptD and LptA.

N-LptD belongs to the same OstA structural superfamily as LptA and LptC,^{25,27,28} but its three-dimensional structure is unknown. We generated a homology-based structural model for N-LptD (Figure 2C) and probed whether the interactions between N-LptD and LptA resemble those between LptC and LptA. To do this, we incorporated pBPA at 22 positions throughout the N-terminal domain of a full-length, functional LptD. Indeed, LptD and LptA could be cross-linked when pBPA was incorporated at several positions at the N-terminal edge of the predicted β -jellyroll of N-LptD (Figure 2C,F and Figure S3 of the Supporting Information). These results show that the N-terminal edge of N-LptD interacts with the C-terminal edge of LptA. Therefore, all three OstA superfamily domains interact in a similar, ordered fashion, with the N- and C-termini of each domain oriented toward the IM and OM, respectively.

It has been proposed that LptA may function as an oligomer on the basis of its crystal structure,²⁵ and concentration-dependent head-to-tail oligomerization of LptA in vitro has been reported.²⁹ However, it is not known whether LptA oligomers exist in vivo. When we coexpressed FLAG-tagged LptA (LptA-FLAG) with pBPA-substituted LptA-His, we observed UV-dependent covalent LptA dimers in vivo. The residues involved in this interaction were found at the N- and C-terminal edges of the LptA β -jellyroll (Figure S4A,B of the Supporting Information), consistent with the LptA crystal structure²⁵ and in vitro chemical cross-linking data.²⁹ In particular, residue H37 at the N-terminal edge of LptA can participate in both homodimerization and heterodimerization with LptC (Figure 2A), whereas residue V163 at the C-terminal edge of LptA can participate in both homodimerization and heterodimerization with LptD (Figure 2D). Therefore, LptA can form head-to-tail homodimers in vivo. Nevertheless, it is also possible that a single LptA molecule can bridge the periplasm by contacting both LptC and N-LptD.

Assembly of the Lpt Bridge Requires the Presence of Native Disulfide Bonds in LptD. The OM translocon is composed of the transmembrane β -barrel protein LptD and the lipoprotein LptE.^{14,15} In the functional translocon, LptE resides within the lumen of the LptD β -barrel.¹⁶ In the absence of LptE, LptD cannot form the two nonconsecutive, interdomain disulfide bonds, C31–C724 and C173–C725, at least one of which must be present for LptD to function.¹⁷ Defects in any Lpt component lead to the buildup of LPS in the IM; therefore, transport across the periplasm and the OM is somehow coupled to prevent LPS mistargeting. We reasoned that the cell may accomplish this by coordinating the assembly of the Lpt bridge with that of the LptD–LptE translocon. One possibility is that assembly of the transenvelope bridge is required for the formation of correct disulfide bonds in LptD. In this case, assembly of the active OM translocon would require two distinct signals: the presence of LptE and that of an intact transenvelope bridge. Disrupting the bridge should then compromise the formation of correct LptD disulfide bonds.

To test this possibility, we constructed a series of 10 mutant LptD proteins lacking specific portions of the LptA-binding site in N-LptD (Figures 2C,F and 3A). Progressively larger deletions

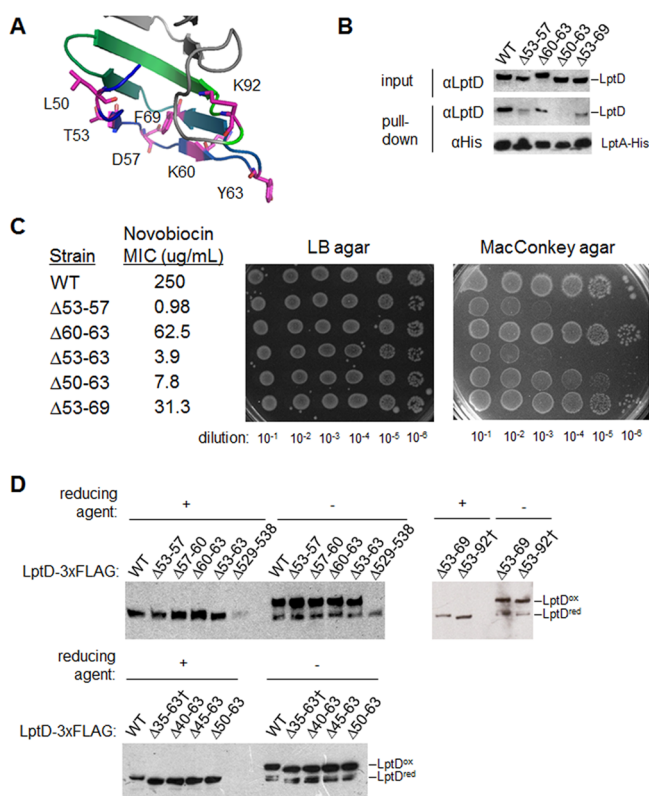


Figure 3. The OM translocon can form in a manner independent of the transenvelope bridge. (A) Model structure of the N-terminal domain of LptD (see Figure 2C), magnified to highlight the LptA-interacting residues (see Figure 2F and Figure S3 of the Supporting Information). (B) Membrane extracts from chromosomal $\Delta lptD::kan$ cells expressing LptA-His and the indicated variant of LptD were analyzed by SDS-PAGE and immunoblotting with the indicated antibodies, either before (input) or after TALON affinity chromatography. (C) The OM integrity of chromosomal $\Delta lptD::kan$ cells expressing the indicated *lptD* variants was tested by determination of the minimal inhibitory concentration (MIC) of novobiocin in LB media and by serial dilution onto either LB agar or MacConkey agar. (D) Total lysates from cells expressing the indicated variant of LptD-3xFLAG were analyzed by SDS-PAGE in the presence or absence of the reducing agent β -mercaptoethanol, followed by immunoblotting with the α FLAG antibody. The correctly oxidized form of LptD, LptD^{ox}, migrates at a higher apparent molecular mass than the reduced form, LptD^{red} (ref 17). The previously characterized $\Delta 529-538$ variant is an example of an incorrectly oxidized mutant protein.¹⁶ The dagger denotes nonfunctional LptD variants.

in this region decreased the affinity of LptD for LptA-His, confirming the importance of these residues in LptD–LptA interactions (Figure 3B). In cells, small- to moderate-sized deletions (e.g., $\Delta 53-57$ and $\Delta 53-63$) compromised the integrity of the OM, as judged by its cellular sensitivity to MacConkey agar and novobiocin (Figure 3C),⁴ whereas large deletions ($\Delta 35-63$ and $\Delta 53-92$) led to a loss of cell viability (not shown), consistent with the role of these residues in forming the transenvelope bridge. However, all the deletion mutant proteins, even those with a complete loss of function, still adopted a wild-type-like disulfide bond configuration (Figure 3D). Therefore, the ability to form a transenvelope bridge is not necessary for LptD to form the correct disulfide bonds.

An alternative possibility is that proper assembly of LptD disulfides is a prerequisite for formation of the Lpt bridge. To test this hypothesis, we used several different LptD mutant

proteins that each contained only one disulfide bond. Wild-type LptD contains four cysteine residues at positions 31, 173, 724, and 725 (denoted CCCC); in each mutant, two of these were replaced with serine (S). Like wild-type LptD, each of these mutant variants could still associate with LptE (Figure 4A and Figure S5A of the Supporting Information), showing that these proteins are stably expressed and correctly folded and inserted into the OM. The SCSC protein can support cell viability because it contains a C173–C725 disulfide bond, one of the two disulfides found in wild-type LptD; by contrast, the other three variants (CCSS, SSSC, and SSSS) cannot form either of the two native disulfide bonds and are nonfunctional.¹⁷

To determine which of these mutant LptD proteins could associate with LptA, we used LptA-HisV163pBPA, the LptA variant that photo-cross-links to wild-type LptD (Figure 2D). We found that only the SCSC variant could be cross-linked by LptA, whereas the CCSS, SSSC, and SSSS variants could not (Figure 4B). Notably, the SSSS mutant could not interact with LptA despite the presence of a C173–C724 disulfide bond (Figure S5B of the Supporting Information), which differs by only one residue from the C173–C725 configuration found in the functional SCSC mutant. These results show that native disulfide bonds are required for LptD to interact with LptA, explaining why mutant LptD proteins that lack these bonds are nonfunctional. We also tested LptD $\Delta 529-538$, which contains all four cysteine residues but fails to form native disulfide bonds because of a defect in interaction with LptE;¹⁶ this mutant also could not be cross-linked by LptA-His-V163pBPA (Figure S5C of the Supporting Information). Taken together, these results indicate that LptD must adopt a functional disulfide bond configuration before the transenvelope bridge can be assembled.

On the basis of our study of the LptD–LptA interaction (Figure 2D–F), we had expected that N-LptD would contain all the structural determinants necessary for LptA binding. However, our finding that LptA cannot cross-link to incorrectly disulfide-bonded variants of full-length LptD (Figure 4B) indicates that N-LptD must also be properly connected to C-LptD to form the bridge. We imagined that correct disulfide bonds might confer an N-LptD conformation that allows LptA binding. If so, N-LptD should not be capable of interacting with LptA if expressed separately from C-LptD (i.e., as “isolated N-LptD”). Surprisingly, however, we found that isolated N-LptD could be cross-linked by LptA-His-V163pBPA (Figure 4C). This interaction was specific, because isolated C-LptD could not be cross-linked despite being expressed at a far higher level (Figure 4C and Figure S5D of the Supporting Information); also, an LptA-His variant substituted with pBPA at position Y114, away from the C-terminal edge of LptA (Figure 2C), could not be cross-linked to isolated N-LptD (Figure S5E of the Supporting Information). These results show that isolated N-LptD can fold into a conformation that contains the key structural features for LptA binding, despite the absence of native disulfide bonds. The fact that LptA cannot interact with the N-terminal domain of a full-length LptD protein lacking correct disulfide bonds (Figure 4B and Figure S5C of the Supporting Information) suggests that, in full-length LptD, C-LptD prevents N-LptD from binding to LptA until the correct disulfide bonds are established.

DISCUSSION

We have defined the architecture of the transenvelope bridge responsible for the transport of LPS across the periplasm, as well as a regulatory mechanism for controlling bridge assembly

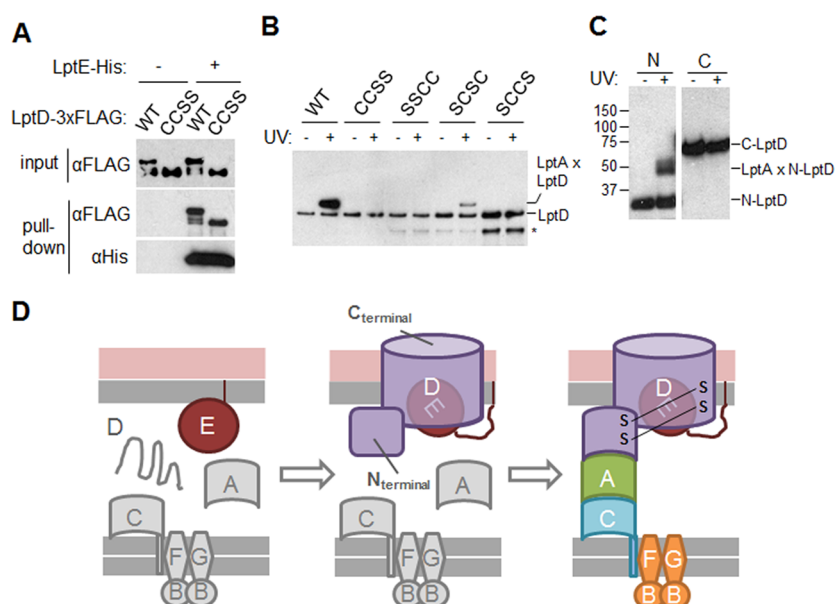


Figure 4. Formation of the transenvelope bridge requires a fully assembled OM translocon. (A) Lysates from cells expressing the indicated variant of LptD-3xFLAG with or without LptE-His were analyzed by nonreducing SDS–PAGE and immunoblotting with the indicated antibodies, either before (input) or after (pull-down) nickel affinity chromatography. C (cysteine) and S (serine) represent the residues present at positions 31, 173, 724, and 725 of LptD. See Figure S5A of the Supporting Information. (B) Cells expressing LptA-His-V163pBPA and the indicated variant of LptD-3xFLAG (labeled as in panel A) were analyzed as described in the legend of Figure 2A and immunoblotted with the α FLAG antibody. To facilitate visualization of both cross-linked and free LptD, this experiment was performed under conditions in which LptD-3xFLAG is retained nonspecifically on nickel resin. The asterisk denotes degradation products of LptD-3xFLAG. See Figure S5B,C of the Supporting Information. (C) Cells expressing LptA-His-V163pBPA and either N-LptD-3xFLAG (amino acids 1–203) or C-LptD-3xFLAG (see Figure 2E) were analyzed as described in the legend of Figure 2A and immunoblotted with the α FLAG antibody. See Figure S5D,E of the Supporting Information. (D) Ordered assembly of the Lpt machinery. Proper association of LptD with LptE is required for folding and insertion of the LptD β -barrel into the OM (first step) and for formation of native disulfide bonds in LptD (second step).^{15–17} The presence of native disulfides in turn permits the N-terminal domain of LptD to engage LptA, allowing the formation of the transenvelope bridge. How the LptC–LptA interaction may be regulated is unknown.

in vivo. We have shown how periplasmic LptA contacts both LptC at the IM and the N-terminal domain of LptD at the OM, creating a continuous bridge of antiparallel β -strands between the membranes (Figure 2C). Our results establish the essential role of N-LptD in orchestrating the biogenesis of the transenvelope bridge, which can occur only after the proper assembly of the OM LPS translocon. In this way, the cell synchronizes the assembly of components in the OM and the periplasm, ensuring proper coordination of their function.

Several lines of evidence indicate that the intermolecular contacts we have identified occur in the functional Lpt bridge in vivo. We tested 59 positions throughout LptC, LptA, and N-LptD, each of which belongs to the OstA structural superfamily; without exception, the residues involved in UV photo-cross-linking in vivo were found only at the exposed edges of these β -sheet structures (Figure 2C), in close agreement with the crystallographic LptA oligomer²⁵ and in vitro studies.²⁹ We (Figure 3C) and others^{23,25} have also shown that genetic disruption of these edge regions compromises the assembly and function of the Lpt bridge. The observed N- to C-terminal orientation of the domains within the bridge is consistent with genomic data: many Gram-negative organisms encode predicted fusion proteins containing as many as four OstA superfamily domains.²⁸ Our data do not resolve the number of LptA molecules present in each transenvelope bridge. We can observe LptA dimers (Figure S4A of the Supporting Information), but their physiological relevance is difficult to establish because the regions of the protein involved in dimerization also interact with LptC and LptD. Structural arguments have been used to suggest that four OstA superfamily domains are necessary to span the

width of the periplasm.²⁵ However, the periplasm may be constricted in the vicinity of Lpt bridges; we have previously shown that the entire transenvelope complex is associated with an unusual membrane fraction containing both IM and OM components,²⁰ suggesting that Lpt bridges might exist within zones of membrane adhesion.^{30,31} It is also possible that the transenvelope bridge is not a static structure but can vary in length to accommodate varying intermembrane distances under different cellular conditions or in different organisms.

We have shown that N-LptD performs the essential function of linking the OM translocon to the transenvelope bridge in a regulated manner. The N-terminal domain of a full-length LptD protein can interact with LptA (Figure 2F), but only if at least one native disulfide bond is present within LptD (Figure 4B and Figure S5C of the Supporting Information). The formation of these native disulfides depends on the proper assembly of LptD with LptE.^{15–18} Thus, LptD disulfide bonds report on the presence of a correctly assembled LptD–LptE translocon in the OM, which then allows the formation of the transenvelope bridge (Figure 4D). This regulatory mechanism ensures that the cell does not couple Lpt bridges to nonfunctional OM translocons, consistent with the observation that depletion of LptD or LptE results in LptA degradation²³ and causes LPS to accumulate at the IM.⁹ The presence of active transenvelope bridges coupled to defective OM translocons might be harmful to the cell because LPS would be mistargeted to the periplasm.

It is intriguing that, in full-length, nonfunctional LptD molecules, the C-terminal β -barrel prevents the N-terminal domain from interacting with LptA: N-LptD can interact with LptA on its own (Figure 4C), but not in the context of a full-length

LptD molecule lacking correct disulfide bonds (Figure 4B and Figure S5C of the Supporting Information). LptD is one of the largest OM β -barrels, predicted to contain as many as 24 β -strands.^{32,33} Every structurally characterized β -barrel protein of this size is occluded by a plug domain encoded on the same polypeptide.³⁴ Previously, we established that mature LptD is plugged by a separate protein, LptE.¹⁶ However, these two proteins are assembled at the OM by distinct pathways: the β -barrel assembly pathway³⁵ and the localization of lipoprotein system,³⁶ respectively. Details of how LptD and LptE form a complex remain to be elucidated. Here, we have found that N-LptD is not accessible until LptE properly associates with the C-LptD β -barrel and allows the formation of correct disulfide bonds (Figure 4D).¹⁷ A regulatory mechanism of this type has been demonstrated for the pilus usher FimD: in the presence of a substrate, a plug domain found near the N-terminus of FimD rotates out of the lumen of the FimD β -barrel, opening the channel for translocation of pilus subunits.³⁷

Whereas Gram-negative pathogenesis and virulence can require numerous transenvelope complexes such as efflux pumps and protein secretion machines,^{38,39} the Lpt proteins constitute the only such complex known to be essential for Gram-negative cell viability. A recently discovered *Pseudomonas*-specific peptidomimetic antibiotic binds to LptD, and resistance is conferred by a mutation in the N-terminal domain of *Pseudomonas aeruginosa* LptD.⁴⁰ It is tempting to speculate that this drug disrupts the function or regulation of the transenvelope Lpt bridge in *Pseudomonas*. Understanding the assembly of the Lpt machinery can shed light on how its components function in transporting LPS and how these functions can be disrupted by antibiotics.

■ ASSOCIATED CONTENT

Supporting Information

Additional experimental procedures and supporting data. This material is available free of charge via the Internet at <http://pubs.acs.org>.

■ AUTHOR INFORMATION

Corresponding Author

*E-mail: kahne@chemistry.harvard.edu. Telephone: (617) 496-0215.

Funding

This work was supported by National Institute of Allergy and Infectious Diseases Grant AI081059 (D.K.). E.F. was a graduate fellow of the Fannie and John Hertz Foundation.

Notes

The authors declare no competing financial interest.

■ ACKNOWLEDGMENTS

Plasmid pSup-BpaRS-6TRN was a generous gift from Prof. Peter G. Schultz (The Scripps Research Institute, La Jolla, CA). We thank Z. Yao for MIC measurements, R. M. Davis for technical assistance in generating the Δ *lptA::kan* allele, and Dr. S.-S. Chng, Dr. L. S. Gronenberg, M. Xue, and C. Liu for reagents.

■ REFERENCES

(1) Kamio, Y., and Nikaido, H. (1976) Outer membrane of *Salmonella typhimurium*: Accessibility of phospholipid headgroups to phospholipase C and cyanogen bromide activated dextran in the external medium. *Biochemistry* 15, 2561–2570.

(2) Funahara, Y., and Nikaido, H. (1980) Asymmetric localization of lipopolysaccharides on the outer membrane of *Salmonella typhimurium*. *J. Bacteriol.* 141, 1463–1465.

(3) Mühlradt, P. F., and Golecki, J. R. (1975) Asymmetrical distribution and artefactual reorientation of lipopolysaccharide in the outer membrane bilayer of *Salmonella typhimurium*. *Eur. J. Biochem.* 51, 343–352.

(4) Nikaido, H. (2003) Molecular basis of bacterial outer membrane permeability revisited. *Microbiol. Mol. Biol. Rev.* 67, 593–656.

(5) Raetz, C. R., and Whitfield, C. (2002) Lipopolysaccharide endotoxins. *Annu. Rev. Biochem.* 71, 635–700.

(6) Doerfler, W. T. (2006) Lipid trafficking to the outer membrane of Gram-negative bacteria. *Mol. Microbiol.* 60, 542–552.

(7) Sperandio, P., Dehò, G., and Polissi, A. (2009) The lipopolysaccharide transport system of Gram-negative bacteria. *Biochim. Biophys. Acta* 1791, 594–602.

(8) Sperandio, P., et al. (2007) Characterization of *lptA* and *lptB*, two essential genes implicated in lipopolysaccharide transport to the outer membrane of *Escherichia coli*. *J. Bacteriol.* 189, 244–253.

(9) Sperandio, P., et al. (2008) Functional analysis of the protein machinery required for transport of lipopolysaccharide to the outer membrane of *Escherichia coli*. *J. Bacteriol.* 190, 460–4469.

(10) Ruiz, N., Gronenberg, L. S., Kahne, D., and Silhavy, T. J. (2008) Identification of two inner-membrane proteins required for the transport of lipopolysaccharide to the outer membrane of *Escherichia coli*. *Proc. Natl. Acad. Sci. U.S.A.* 105, 5537–5542.

(11) Narita, S., and Tokuda, H. (2009) Biochemical characterization of an ABC transporter LptBFGC complex required for the outer membrane sorting of lipopolysaccharides. *FEBS Lett.* 583, 2160–2164.

(12) Braun, M., and Silhavy, T. J. (2002) Imp/OstA is required for cell envelope biogenesis in *Escherichia coli*. *Mol. Microbiol.* 45, 1289–1302.

(13) Bos, M. P., Tefsen, B., Geurtsen, J., and Tommassen, J. (2004) Identification of an outer membrane protein required for the transport of lipopolysaccharide to the bacterial cell surface. *Proc. Natl. Acad. Sci. U.S.A.* 101, 9417–9422.

(14) Wu, T., et al. (2006) Identification of a protein complex that assembles lipopolysaccharide in the outer membrane of *Escherichia coli*. *Proc. Natl. Acad. Sci. U.S.A.* 103, 11754–11759.

(15) Chng, S. S., Ruiz, N., Chimalakonda, G., Silhavy, T. J., and Kahne, D. (2010) Characterization of the two-protein complex in *Escherichia coli* responsible for lipopolysaccharide assembly at the outer membrane. *Proc. Natl. Acad. Sci. U.S.A.* 107, 5363–5368.

(16) Freinkman, E., Chng, S. S., and Kahne, D. (2011) The complex that inserts lipopolysaccharide into the bacterial outer membrane forms a two-protein plug-and-barrel. *Proc. Natl. Acad. Sci. U.S.A.* 108, 2486–2491.

(17) Ruiz, N., Chng, S. S., Hiniker, A., Kahne, D., and Silhavy, T. J. (2010) Nonconsecutive disulfide bond formation in an essential integral outer membrane protein. *Proc. Natl. Acad. Sci. U.S.A.* 107, 12245–12250.

(18) Chimalakonda, G., et al. (2011) Lipoprotein LptE is required for the assembly of LptD by the β -barrel assembly machine in the outer membrane of *Escherichia coli*. *Proc. Natl. Acad. Sci. U.S.A.* 108, 2492–2497.

(19) Tefsen, B., Geurtsen, J., Beckers, F., Tommassen, J., and de Cock, H. (2005) Lipopolysaccharide transport to the bacterial outer membrane in spheroplasts. *J. Biol. Chem.* 280, 4504–4509.

(20) Chng, S. S., Gronenberg, L. S., and Kahne, D. (2010) Proteins required for lipopolysaccharide assembly in *Escherichia coli* form a transenvelope complex. *Biochemistry* 49, 4565–4567.

(21) Chin, J. W., and Schultz, P. G. (2002) In vivo photocrosslinking with unnatural amino acid mutagenesis. *ChemBioChem* 11, 1135–1137.

(22) Liu, C. C., and Schultz, P. G. (2010) Adding new chemistries to the genetic code. *Annu. Rev. Biochem.* 79, 413–444.

(23) Sperandio, P., et al. (2011) New insights into the Lpt machinery for lipopolysaccharide transport to the cell surface: LptA-

LptC interaction and LptA stability as sensors of a properly assembled transenvelope complex. *J. Bacteriol.* 193, 1042–1053.

(24) Bowyer, A., Baardsnes, J., Ajamian, E., Zhang, L., and Cygler, M. (2011) Characterization of interactions between LPS transport proteins of the Lpt system. *Biochem. Biophys. Res. Commun.* 40, 1093–1098.

(25) Suits, M. D., Sperandio, P., Dehò, G., Polissi, A., and Jia, Z. (2008) Novel structure of the conserved Gram-negative lipopolysaccharide transport protein A and mutagenesis analysis. *J. Mol. Biol.* 380, 476–488.

(26) Tran, A. X., Dong, C., and Whitfield, C. (2010) Structure and functional analysis of LptC, a conserved membrane protein involved in the lipopolysaccharide export pathway in *Escherichia coli*. *J. Biol. Chem.* 285, 33529–33539.

(27) Bos, M. P., Robert, V., and Tommassen, J. (2007) Biogenesis of the Gram-negative bacterial outer membrane. *Annu. Rev. Microbiol.* 61, 191–214.

(28) Finn, R. D., et al. (2008) The Pfam protein families database. *Nucleic Acids Res.* 36, D281–D288.

(29) Merten, J. A., Schultz, K. M., and Klug, C. S. (2012) Concentration-dependent oligomerization and oligomeric arrangement of LptA. *Protein Sci.* 21, 211–218.

(30) Bayer, M. E. (1968) Areas of adhesion between wall and membrane of *Escherichia coli*. *J. Gen. Microbiol.* 53, 395–404.

(31) Bayer, M. E. (1991) Zones of membrane adhesion in the cryofixed envelope of *Escherichia coli*. *J. Struct. Biol.* 107, 268–280.

(32) Bagos, P. G., Liakopoulos, T. D., Spyropoulos, I. C., and Hamodrakas, S. J. (2004) PRED-TMBB: A web server for predicting the topology of β -barrel outer membrane proteins. *Nucleic Acids Res.* 32, W400–W404.

(33) Hayat, S., and Elofsson, A. (2012) BOCTOPUS: Improved topology prediction of transmembrane β barrel proteins. *Bioinformatics* 28, 516–522.

(34) Fairman, J. W., Noinaj, N., and Buchanan, S. K. (2011) The structural biology of β -barrel membrane proteins: A summary of recent reports. *Curr. Opin. Struct. Biol.* 21, 523–531.

(35) Hagan, C. L., Silhavy, T. J., and Kahne, D. (2011) β -Barrel membrane protein assembly by the Bam complex. *Annu. Rev. Biochem.* 80, 189–210.

(36) Okuda, S., and Tokuda, H. (2011) Lipoprotein sorting in bacteria. *Annu. Rev. Microbiol.* 65, 239–259.

(37) Phan, G., et al. (2011) Crystal structure of the FimD usher bound to its cognate FimC-FimH substrate. *Nature* 474, 49–53.

(38) Misra, R., and Bavro, V. N. (2009) Assembly and transport mechanism of tripartite drug efflux systems. *Biochim. Biophys. Acta* 1794, 817–825.

(39) Holland, I. B. (2010) The extraordinary diversity of bacterial protein secretion mechanisms. In *Protein Secretion* (Economou, A., Ed.) Methods in Molecular Biology, Vol. 619, pp 1–20, Springer, New York.

(40) Srinivas, N., et al. (2010) Peptidomimetic antibiotics target outer-membrane biogenesis in *Pseudomonas aeruginosa*. *Science* 327, 1010–1013.

(41) Söding, J., Biegert, A., and Lupas, A. N. (2005) The HHpred interactive server for protein homology detection and structure prediction. *Nucleic Acids Res.* 33, W244–W248.